

Focal Temporal Scleral Bulge with Choroidal Thinning: An Under-Recognized Tomographic Feature

Rosa Dolz-Marco^{1*}, Roberto Gallego-Pinazo¹, Maria Isabel López-Gálvez², Jose I Tembl³, Manuel Díaz-Llopis⁴ and Carol Shields⁵

¹Department of Ophthalmology, University and Polytechnic Hospital La Fe, Valencia, Spain

²Department of Ophthalmology, Hospital Clínico Universitario de Valladolid, Valladolid, Spain

³Department of Neurology, University and Polytechnic Hospital La Fe, Valencia, Spain

⁴Faculty of Medicine, University of Valencia

⁵Ocular Oncology Service Wills Eye Hospital, Thomas Jefferson University, Philadelphia, PA, United States of America (USA)

*Corresponding author: Rosa Dolz-Marco, Department of Ophthalmology, University and Polytechnic Hospital La Fe. Bulevar Sur s/n. 46026, Valencia, Spain, Tel: 0034 650314806; Email: rosadolzmarco@gmail.com

Received date: Feb 05, 2015, Accepted date: Apr 15, 2015, Published date: Apr 20, 2015

Copyright: © 2015 Dolz-Marco R, et al. This is an open-access article distributed under the terms of the Creative Commons Attribution License, which permits unrestricted use, distribution, and reproduction in any medium, provided the original author and source are credited.

Abstract

Purpose: To describe the swept source tomographic characteristics of focal temporal scleral bulge with choroidal thinning as a normal variation of the ocular anatomy in healthy eyes.

Methods: Cross-sectional observational study. Swept-source optical coherence tomography (SS-OCT) examinations in healthy patients performed between October and December 2013 were analyzed. The presence of a focal scleral bulge with choroidal thickness (CT) variation was evaluated. In those cases with this finding we manually measured the extension of the scleral protuberance and the choroidal shape.

Results: There were 166 eyes of 106 patients analyzed and 13% (22 eyes of 16 patients) demonstrated a focal scleral bulge. The scleral bulge was not visible ophthalmoscopically in any case. By SS-OCT, the scleral bulge had a mean basal diameter of 3225 microns (range 1954-4908 microns) and mean distance temporal to the foveola of 2261 microns (range 1148-4173 microns). Compared to normal submacular scleral thickness, the temporal scleral bulge was a mean of 107 microns thicker (range 31-171 microns). The mean overlying choroidal thickness was 177 microns (range 79-326 microns) compared with mean subfoveal thickness in the involved eye of 250 microns (range 99-431 microns), mean thickness at temporal edge of the bulge of 312 microns (range 195-529 microns). The overlying retinal pigment epithelium and inner retinal contour were normal in all cases.

Conclusions: On SS-OCT, 13% of healthy eyes showed temporal scleral bulge with related choroidal thinning. The clinical significance of this novel sign is under evaluation.

Keywords: Choroid thinning; Sclera bulge; Macula; Inferior oblique muscle; Swept-source OCT

Introduction

The choroid is a highly vascular layer of the eye, limited anteriorly by the retinal pigment epithelium (RPE) and posteriorly by the sclera. This tissue provides oxygen and nutrition to the outer retina, the retinal pigment epithelium (RPE) and the prelaminar portion of the optic nerve [1]. The choroid has been classically visualized by fluorescein and indocyanine green angiography. Choroidal thickness (CT) has been measured by ultrasound and magnetic resonance imaging, but with marked limitations due to poor resolution of imaging techniques [2-3]. Optical coherence tomography (OCT), and particularly, enhanced depth imaging (EDI-OCT) and swept source (SS-OCT) have improved resolution of the choroidal details with capability of precise measurement up to 6 microns [4-6].

There are several reported factors that can influence CT including diurnal fluctuations, [7] typically greater in men, increasing age, and increasing axial length [8-10]. Regarding diurnal variation, the choroid was found to be most congested with increased thickness at 8 am and

thinnest at 5 pm [7]. Margolis et al established that each increasing decade of life was correlated with subfoveal CT decrease by approximately 15.6 microns [9]. Flores-Moreno et al suggested that each increasing mm in axial length was correlated with subfoveal CT decrease by 25.9 microns [10]. In addition, systemic and ocular characteristics have been reported to increase CT such as water drinking [11], sildenafil citrate [12], hypercholesterolemia [13], central serous chorioretinopathy [14], and inflammatory ophthalmic diseases including Vogt Koyanagi Harada syndrome [15], and posterior scleritis [16]. Decrease of CT was found with oral intake of nicotine [17] and coffee [18]. Pupillary dilation does not modify CT [19].

Several authors have studied the topographic distribution of CT within the macular area of normal eyes using various OCT devices and demonstrated marked asymmetry within the macular area [9,20-23]. The thickest CT corresponded with the subfoveal area, decreasing rapidly in the nasal direction. CT was evidenced thicker temporally than nasally, and thicker superiorly than inferiorly.

Using SS-OCT we have recently observed a novel OCT finding in the temporal macular region, characterized by scleral inward bulge accompanied by focal choroidal thinning [24]. Herein, we report the

quantitative and qualitative analysis of this finding in healthy patients analyzed using SS-OCT.

Methods

We performed a cross-sectional non-randomized observational study to evaluate the submacular choroid and sclera of clinically normal eyes that underwent high-penetrance OCT exam (SS-OCT, DRI Atlantis, Topcon Medical, Oakland, NJ, USA) between October 2013 and December 2013 at the Unit of Macula of the University and Polytechnic Hospital La Fe, Valencia, Spain.

The patient demographic and clinical data were collected including age, gender, and axial length (AL). Two different scan protocols of the SS-OCT were used including the posterior pole 3D cube (12 × 9 mm;

512 horizontal A-scans x 256 vertical A-scans) and the high-definition 12 mm radial scan (12 scans).

The SS-OCT scans with evidence of focal temporal scleral bulge with choroidal thinning were further analyzed by a single investigator (RDM). Eyes with clinically-evident macular pathology such as vascular diseases, pathologic myopia (more than 6 diopters), or posterior uveitis were excluded from analysis. In addition, eyes without poor or incomplete visualization of the sclerochoroidal boundary were excluded to avoid misinterpretation of data.

The scleral bulge was identified by the inward bowing on SS-OCT and different parameters were manually measured as depicted in Figure 1.

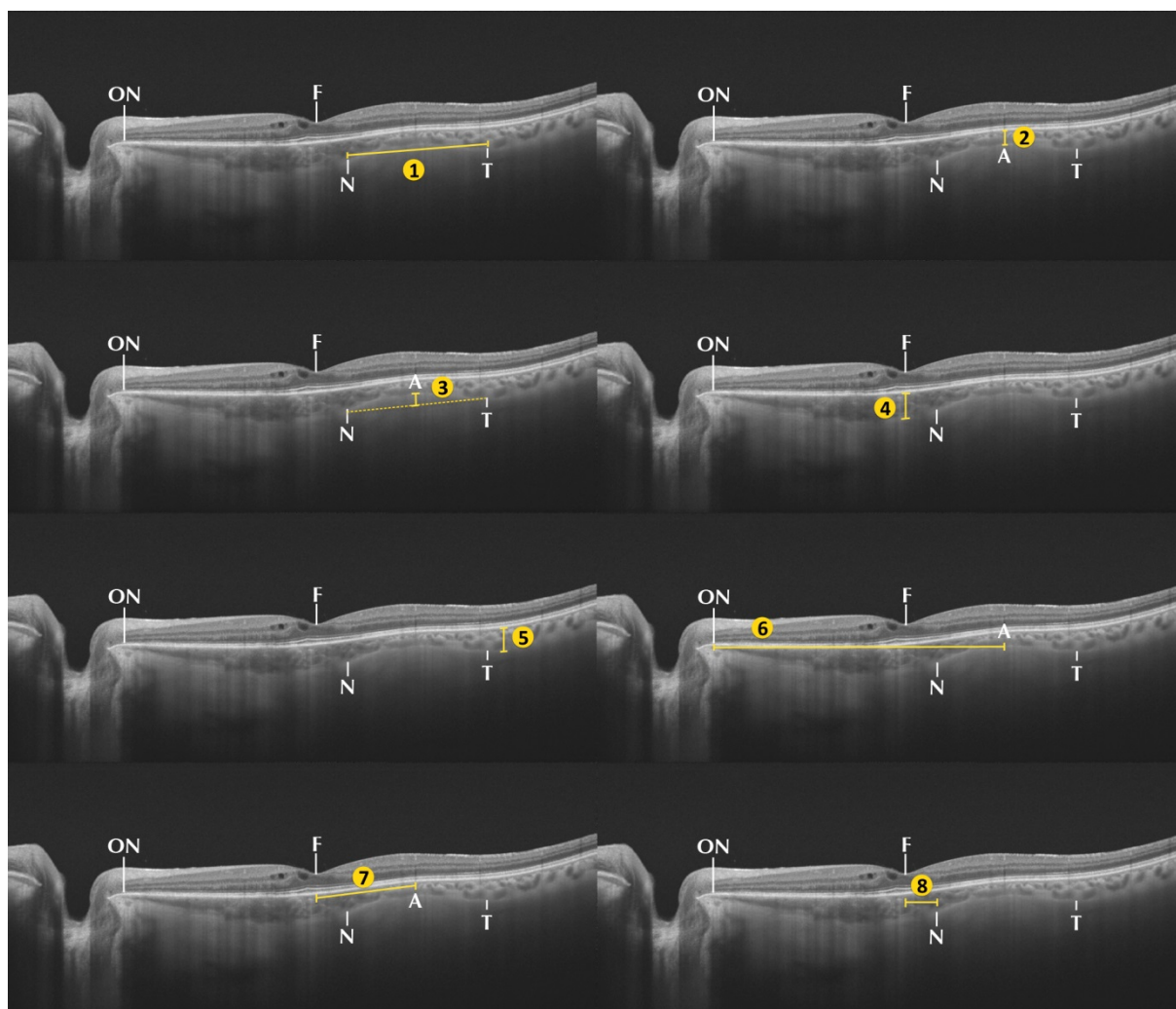


Figure 1: Schema of the different characteristics manually measured in each case. 1. Extension of the choroidal thinning in the horizontal axis (distance between both the nasal -N- and the temporal -T- limit of the scleral bulge); 2. Minimum choroidal thickness (CT) at the apex of the scleral bulge (A); 3. Scleral elevation at the level of minimum CT; 4. Subfoveal CT; 5. Maximum temporal CT; 6. Distance from the point of minimum CT to the temporal edge of the optic nerve (ON). 7. Distance from the point of minimum CT to the foveola (F); and 8. Distance of the nasal limit of the choroidal thinning to the foveola.

The various measurements assessed included the maximum scleral elevation at the apex of the scleral bulge (distance between the

innermost and the outermost point of the sclero-choroidal junction); the basal dimension of the scleral bulge in the horizontal axis (distance

between both the nasal and the temporal limit of the scleral bulge); the distance from the apex of the scleral bulge to the foveola (measured from the point of minimum CT); the distance of the nasal margin of the scleral bulge to the foveola; and the distance from the apex of the scleral bulge to the temporal edge of the optic nerve (measured from the point of minimum CT) were also assessed. We also analyzed the minimum CT (measured at the apex of the scleral bulge); the subfoveal CT and the maximum temporal CT (evaluated temporal to the area of choroidal thinning). The location of the nasal edge of the scleral bulge (temporal to the foveola, subfoveal or nasal to the foveola) was also evaluated. The contour of the RPE and the inner retina were also analyzed.

In addition, analysis of the qualitative characteristics of the color fundus photographs, fluorescein angiography and/or indocyanine green angiography for correlation with the SS-OCT findings was performed.

Feature	Eyes with scleral bulge N=22 eyes of 16 patients	Eyes without scleral bulge N=144 eyes of 90 patients	p-value	Total N=166 eyes of 106 patients
Gender				
Male	8	37	<0.001	45
Female	8	53	<0.001	61
Age (mean, median, range) years	58, 58, 20-85	47, 45, 17-89	0.008	48, 47, 17-89
Globe axial length (mean, median, range) mm	24, 24, 22-25	24, 24, 21-28	0.620	24, 24, 21-28

Table 1: Temporal scleral bulge with choroidal thinning in 166 normal eyes. Patient demographics.

Characteristics of the focal temporal scleral bulge with choroidal thinning

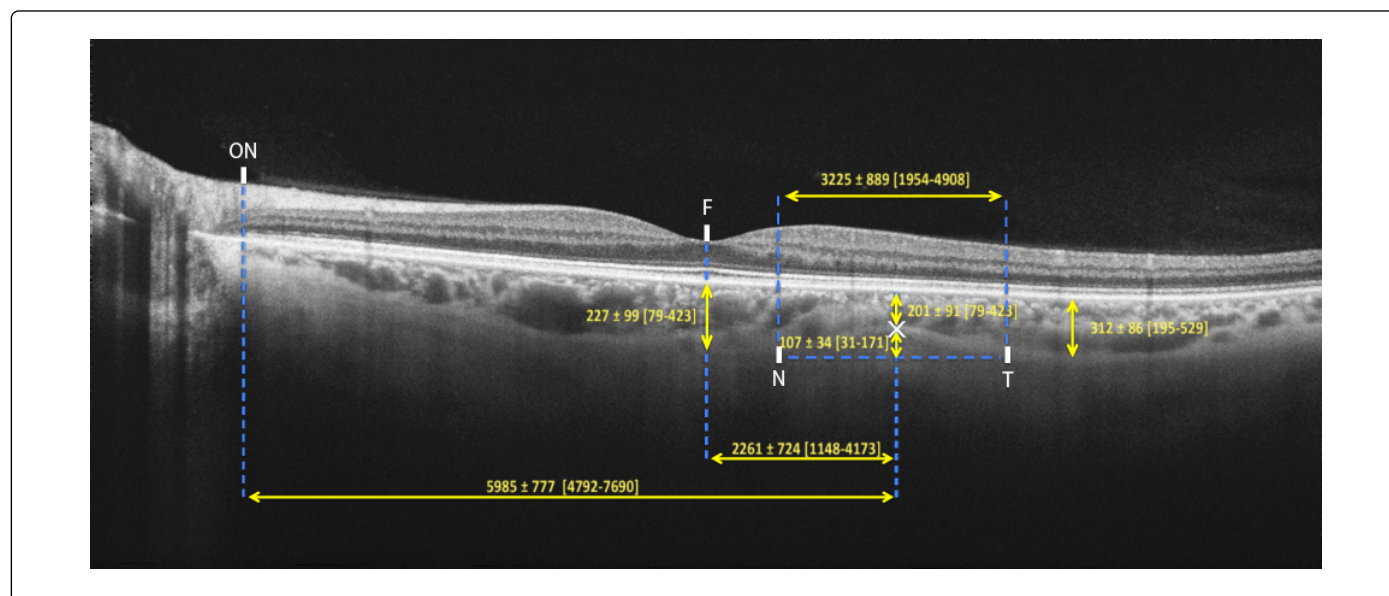


Figure 2: Mean measures of the main features manually measured in our case series expressed in microns.

The tomographic characteristics of the focal temporal scleral bulge with choroidal thinning are represented in Figure 2 and summarized

Results

General population and demographic data

Demographic data are summarized in Table 1. A total number of 173 healthy eyes of 111 patients were evaluated by SS-OCT in this study. Seven eyes of 5 patients were excluded due to an incomplete visualization of the sclerochoroidal boundary. Therefore, 166 healthy eyes of 106 patients (43 men and 58 women) were included for the final analysis of the SS-OCT scans. The mean age was 48 ± 19 years [range: 17-89] and the mean AL was 24 ± 1.4 mm. There were 22 eyes of 16 patients showing a focal temporal scleral bulge with choroidal thinning, thus the prevalence of this finding in our study sample was 13%.

in Table 2. The mean scleral elevation at the apex of the scleral bulge was 107 ± 34 microns [range: 31-171] with a mean extension of the choroidal bulge in the horizontal axis was 3225 ± 889 microns [range: 1954-4908]. The mean CT at the apex of the scleral bulge was 177 ± 76 microns [range: 79-326] and the mean subfoveal CT was 250

± 98 microns [range: 99-431]. The focal choroidal thinning was found in the temporal area in all cases, although the nasal edge of the scleral bulge was found temporal to the foveola in 17 eyes (77%); in the subfoveal region in 3 eyes (14%); and nasal to the foveola in 2 eyes

(9%). The RPE contour and the inner retinal contour were normal in all cases. No apparent sign in the biomicroscopic or angiographic evaluation of the fundus were associated with the SS-OCT finding.

Feature	Eyes with scleral bulge N=22 eyes of 16 patients
Scleral findings, mean \pm SD [range] microns	
Scleral bulge thickness	107 \pm 34 [31-171]
Scleral bulge basal dimension	3225 \pm 889 [1954-4908]
Scleral bulge distance from foveola to apex	2261 \pm 724 [1148-4173]
Scleral bulge distance from foveola to nasal margin	624 \pm 454 [0-1517]
Scleral bulge distance from optic disc to apex	5985 \pm 777 [4792-7690]
Choroidal findings, mean \pm SD [range] microns	
Choroidal thickness at apex	177 \pm 76 [79-326]
Choroidal thickness at temporal margin of scleral bulge	312 \pm 86 [195-529]
Subfoveal choroidal thickness	250 \pm 98 [99-431]
Choroidal thickness at apex scleral bulge c/w subfoveal choroid	74 \pm 52 [30-193]
Location of the nasal edge of the scleral bulge, number (%)	
Temporal to the foveola	17 eyes (77)
Subfoveal	3 eyes (14)
Nasal to the foveola	2 eyes (9)
c/w-compared with	

Table 2: Temporal scleral bulge with choroidal thinning in 166 normal eyes. Tomographic characteristics of the scleral bulge.

Discussion

We report the presence of a focal temporal scleral bulge with choroidal thinning in 13% of the studied normal population (22 eyes of 159 eyes). The main SS-OCT characteristics of this novel finding include: focal scleral protuberance with thinning of the overlying choroidal tissue; lack of changes in the RPE or the inner profile of the retina; location temporal to the foveola (Figure 3).

The topography and variations of CT have been widely reported [9,20-23]. Margolis and Spaide described a progressive thinning of the CT in the horizontal section from the subfoveal to the temporal and nasal regions [9]. Later, Hirata et al. found the choroid to be thicker in the temporal and superior sectors compared with the nasal and inferior regions, [25] and Tan et al recently found similar results [23]. On the other hand, Esmaelpour et al showed that CT variations were more evident in the superior macular region than inferiorly [21].

In the present study, we describe a frequent variation on the macular CT topography with a well-defined thinning constantly evidenced within the temporal macular region when present, with a variable distance to the foveola and a variable extent of the inward scleral bulge. This temporal thinning in choroidal thickness does not evidence any influence in the subfoveal choroidal thickness. Our

results show a mean subfoveal choroidal thickness of 250 \pm 98 microns, in agreement with previous data [25-26]. The origin of this novel finding is unknown. In our series, scleral tissue could not be entirely visualized, thus the involvement of the sclera in the development of this finding is not conclusive. We found a striking similarity of the OCT images of this temporal choroidal thinning with sclerochoroidal calcification as described by Shields et al within the superior macular region [27].

They hypothesized that the chronic tractional forces induced by the superior oblique muscle could play a significant role in the pathogenesis of sclerochoroidal calcification. We consider the possibility that variations in the inferior oblique muscle insertion could progressively cause scleral variation with subsequent choroidal thinning. These variations has been reported by Yalçin et al, showing the presence of double, triple, or multiple muscle bellies in approximately 90% of cases [28]. In addition, patients with this variation in the choroidal distribution seem to be older than the general population ($p=0.008$), suggesting a progressive change with age. Nevertheless, the unremarkable appearance of the fundus examination in our cases is against the hypothesis of calcification of the inferior oblique insertion, as that would likely cause a yellow discoloration of the fundus.

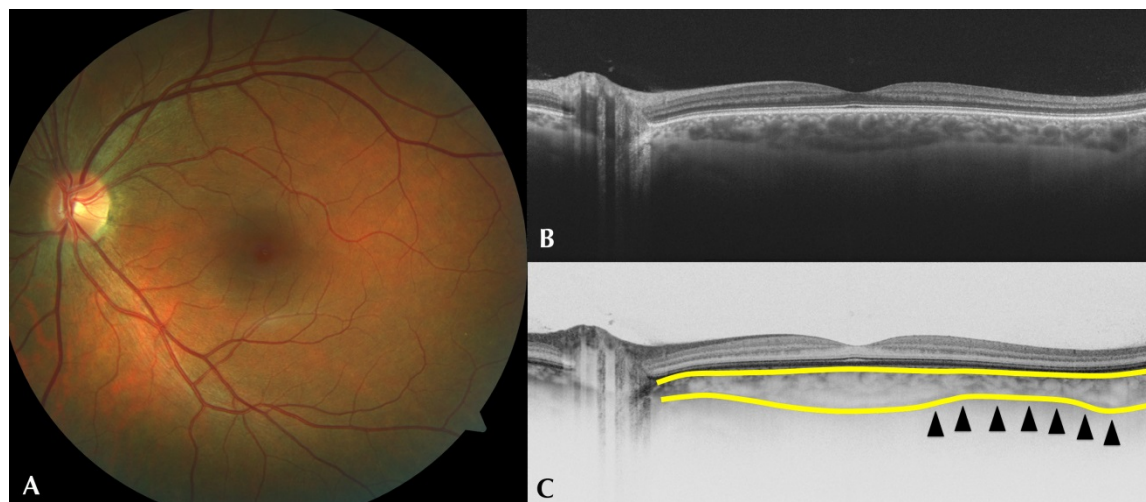


Figure 3: A 20-year-old man with focal temporal decrease of the choroidal thickness. Color fundus photographs (A) demonstrate an unremarkable fundus examination. Optical coherence tomography (OCT) (B-C) demonstrate an inward focal bulge of the sclerochoroidal junction at the temporal macular region (arrowheads), associated with focal thinning of the overlying choroid.

In addition, the mean distance of the insertion of the inferior oblique muscle to the foveola was reported by Siam et al. to be 4500 microns (Figure 4) [29] and the mean distance of the scleral bulge was closer to the fovea in our cases (2261 ± 724 microns) (Figure 2). On the other hand, we have found some cases with a wider extension of the scleral bulge involving the nasal macular area. These features are not explained by the insertion variability of the inferior oblique muscle.

This artery enters the sclera temporal to the fovea at a mean distance of 1500 microns, and the intrascleral course has a mean length of 4000 microns [29]. The location of the TLPCA correlates with the finding we report, but the absence of vascular tracts within the scleral bulge in our images would not support this hypothesis.

In summary, a focal temporal scleral bulge with choroidal thinning was detected in 13% of imaged ophthalmoscopically normal eyes. This novel finding is characterized by a scleral contour modification with no associated involvement of the RPE or the retinal contour, but with frequent anatomic thinning of the overlying CT topography. The limitations of our study include the absence of histopathologic correlation and the lack of an imaging technique that allows better visualization of depth in this anatomic change. Further studies are warranted in order to analyze the origin of this constant and frequent modification of the CT macular topography.

References

1. Mrejen S, Spaide RF (2013) Optical coherence tomography: imaging of the choroid and beyond. *Surv Ophthalmol* 58: 387-429.
2. Townsend KA, Wollstein G, Schuman JS (2008) Clinical application of MRI in ophthalmology. *NMR Biomed* 21: 997-1002.
3. Coleman DJ, Silverman RH, Chabi A, Rondeau MJ, Shung KK, et al. (2004) High-resolution ultrasonic imaging of the posterior segment. *Ophthalmology* 111: 1344-1351.
4. Spaide RF, Koizumi H, Pozzoni MC (2008) Enhanced depth imaging spectral-domain optical coherence tomography. *Am J Ophthalmol* 146: 496-500.
5. Choma M, Sarunic M, Yang C, Izatt J (2003) Sensitivity advantage of swept source and Fourier domain optical coherence tomography. *Opt Express* 11: 2183-2189.
6. Rahman W, Chen FK, Yeoh J, Patel P, Tufail A, et al. (2011) Repeatability of manual subfoveal choroidal thickness measurements in healthy subjects using the technique of enhanced depth imaging optical coherence tomography. *Invest Ophthalmol Vis Sci* 52: 2267-2271.
7. Brown JS, Flitcroft DI, Ying GS, Francis EL, Schmid GF, et al. (2009) In vivo human choroidal thickness measurements: evidence for diurnal fluctuations. *Invest Ophthalmol Vis Sci* 50: 5-12.

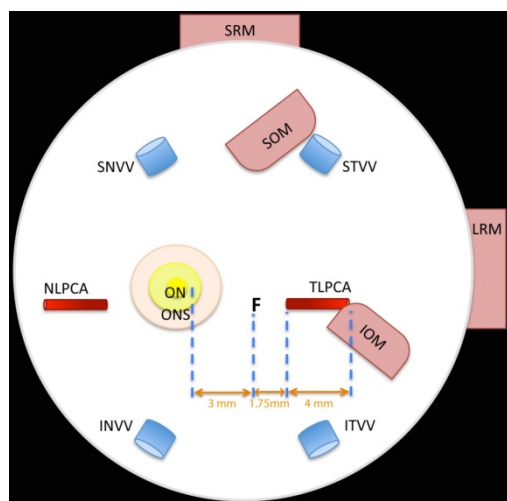


Figure 4: Schema of the distribution of the main structures of the posterior segment adapted from Siam AL et al. "A restudy of the surgical anatomy of the posterior aspect of the globe: an essential topography for exact macular buckling" [29].

Another potential explanation for the presence of this sclerochoroidal modification could be the individual variations of the intrascleral course of temporal long posterior ciliary artery (TLPCA).

8. Lee SW, Yu SY, Seo KH, Kim ES, Kwak HW (2014) Diurnal variation in choroidal thickness in relation to sex, axial length, and baseline choroidal thickness in healthy Korean subjects. *Retina* 34: 385-393.
9. Margolis R, Spaide RF (2009) A pilot study of enhanced depth imaging optical coherence tomography of the choroid in normal eyes. *Am J Ophthalmol* 147: 811-815.
10. Flores-Moreno I, Lugo F, Duker JS, Ruiz-Moreno JM (2013) The relationship between axial length and choroidal thickness in eyes with high myopia. *Am J Ophthalmol* 155: 314-319.
11. Mansouri K, Medeiros FA, Marchase N, Tatham AJ, Auerbach D, et al. (2013) Assessment of choroidal thickness and volume during the water drinking test by swept-source optical coherence tomography. *Ophthalmology* 120: 2508-2516.
12. Vance SK, Imamura Y, Freund KB (2011) The effects of sildenafil citrate on choroidal thickness as determined by enhanced depth imaging optical coherence tomography. *Retina* 31: 332-335.
13. Wong IY, Wong RL, Zhao P, Lai WW (2013) Choroidal thickness in relation to hypercholesterolemia on enhanced depth imaging optical coherence tomography. *Retina* 33: 423-428.
14. Imamura Y, Fujiwara T, Margolis R, Spaide RF (2009) Enhanced depth imaging optical coherence tomography of the choroid in central serous chorioretinopathy. *Retina* 29: 1469-1473.
15. Nakayama M, Keino H, Okada AA, Watanabe T, Taki W, et al. (2012) Enhanced depth imaging optical coherence tomography of the choroid in Vogt-Koyanagi-Harada disease. *Retina* 32: 2061-2069.
16. Uchihori H, Nakai K, Ikuno Y, Gomi F, Hashida N, et al. (2014) Choroidal observations in posterior scleritis using high-penetration optical coherence tomography. *Int Ophthalmol* 34: 937-943.
17. Zengin MO, Cinar E, Kucukerdonmez C (2014) The effect of nicotine on choroidal thickness. *Br J Ophthalmol* 98: 233-237.
18. Vural AD, Kara N, Sayin N, Pirhan D, Ersan HB (2014) Choroidal thickness changes after a single administration of coffee in healthy subjects. *Retina* 34: 1223-1228.
19. Mwanza JC, Sayyad FE, Banitt MR, Budenz DL (2013) Effect of pupil dilation on macular choroidal thickness measured with spectral domain optical coherence tomography in normal and glaucomatous eyes. *Int Ophthalmol* 33: 335-341.
20. Ikuno Y, Kawaguchi K, Nouchi T, Yasuno Y (2010) Choroidal thickness in healthy Japanese subjects. *Invest Ophthalmol Vis Sci* 51: 2173-2176.
21. Esmaeelpour M, Povazay B, Hermann B, Hofer B, Kojic V, et al. (2010) Three-dimensional 1060-nm OCT: choroidal thickness maps in normal subjects and improved posterior segment visualization in cataract patients. *Invest Ophthalmol Vis Sci* 51: 5260-5266.
22. Ouyang Y, Heussen FM, Mokwa N, Walsh AC, Durbin MK, et al. (2011) Spatial distribution of posterior pole choroidal thickness by spectral domain optical coherence tomography. *Invest Ophthalmol Vis Sci* 52: 7019-7026.
23. Tan CS, Cheong KX, Lim LW, Li KZ (2014) Topographic variation of choroidal and retinal thicknesses at the macula in healthy adults. *Br J Ophthalmol* 98: 339-344.
24. Dolz-Marco R, Gallego-Pinazo R, López-Gálvez MI, Díaz-Llopis M, Shields CL (2014) Focal Inferotemporal Scleral Bulge With Choroidal Thinning: A New Observation on High-Penetration Optical Coherence Tomography. *Retina* 35: 600-602.
25. Hirata M, Tsujikawa A, Matsumoto A, Hangai M, Ooto S, et al. (2011) Macular choroidal thickness and volume in normal subjects measured by swept-source optical coherence tomography. *Invest Ophthalmol Vis Sci* 52: 4971-4978.
26. Ikuno Y, Maruko I, Yasuno Y, Miura M, Sekiryu T, et al. (2011) Reproducibility of retinal and choroidal thickness measurements in enhanced depth imaging and high-penetration optical coherence tomography. *Invest Ophthalmol Vis Sci* 52: 5536-5540.
27. Sivalingam A, Shields CL, Shields JA, McNamara JA, Jampol LM, et al. (1991) Idiopathic sclerochoroidal calcification. *Ophthalmology* 98: 720-724.
28. Yalçın B, Ozan H (2005) Insertional pattern of the inferior oblique muscle. *Am J Ophthalmol* 139: 504-508.
29. Siam AL, El-Mamoun TA, Ali MH (2011) A restudy of the surgical anatomy of the posterior aspect of the globe: an essential topography for exact macular buckling. *Retina* 31: 1405-1411.